TM6SF2 overexpression suppresses the proliferation and promotes apoptosis of human hepatocellular carcinoma cells

ZIYOU HUAI[1*], WANYING XUE[1*], XINXIAO JIN[1*], SHIYU PENG[1], WENQIANG XU[1], SHUJING LI[1], HUANFENG HAO[1] and YUANYUAN WANG[1,2]

[1]School of Life Sciences, Bengbu Medical University, Bengbu, Anhui 233030, P.R. China; [2]Anhui Provincial Key Laboratory of Tumor Evolution and Intelligent Diagnosis and Treatment, Bengbu Medical University, Bengbu, Anhui 233030, P.R. China

Received March 12, 2026; Accepted June 18, 2026

DOI: 10.3892/or.2026.9162

Abstract. Transmembrane protein 6 superfamily member 2 (TM6SF2) is a potential tumor suppressor in hepatocellular carcinoma (HCC). At present, the role of TM6SF2 in HCC is poorly studied. The aim of the present study was to elucidate the potential role of TM6SF2 in hepatocellular carcinoma and its associated molecular mechanisms. The correlation between TM6SF2 and HCC progression was assessed using a bioinformatics approach. A TM6SF2-overexpressing Huh-7 cell model was constructed to examine the effects of TM6SF2 on cell proliferation, migration, invasion, cell-cycle distribution, and apoptosis. Gene Ontology and Kyoto Encyclopedia of Genes and Genomes (KEGG) enrichment analyses of differentially expressed genes (DEGs) in the control Vector and TM6SF2 groups were performed using RNA sequencing (RNA-Seq) data. Reverse transcription-quantitative PCR and western blotting were used to verify the expression of candidate DEGs involved in cell cycle regulation and apoptosis. Overexpression of TM6SF2 inhibited HCC cell proliferation, invasion, and migration and promoted apoptosis. TM6SF2 overexpression induced S-phase cell-cycle arrest and promoted apoptosis in Huh-7 cells. RNA-Seq analysis showed that the majority of DEGs were involved in cell growth and biological processes, including the negative regulation of cell growth. KEGG pathway analysis identified the p53 signaling pathway as significantly enriched. Western blot analysis further showed increased levels of phosphorylated p53 and p21, suggesting p53-related molecular changes. These findings suggest that TM6SF2 may exert anti-tumor effects in Huh-7 cells by inducing S-phase cell-cycle arrest and promoting apoptosis. The observed increases in phosphorylated p53 and p21 indicate that p53-related molecular changes may be associated with TM6SF2 overexpression, although this requires further validation.

Correspondence to: Dr Yuanyuan Wang or Dr Huanfeng Hao, School of Life Science, Bengbu Medical University, 2600 Donghai Road, Bengbu, Anhui 233030, P.R. China
E-mail: yuanyuanwang@bbmc.edu.cn
E-mail: haohuanfeng@bbmu.edu.cn

*Contributed equally

Abbreviations: HCC, hepatocellular carcinoma; TM6SF2, transmembrane 6 superfamily member; NAFLD, non-alcoholic fatty liver disease; GO, Gene Ontology; KEGG, Kyoto Encyclopedia of Genes and Genomes; DEGs, differentially expressed genes; LIHC, liver hepatocellular carcinoma; TCGA, The Cancer Genome Atlas; RT-qPCR, reverse-transcription-quantitative PCR; FPKM, Fragments per Kilobase of transcript sequence per Millions base pairs sequenced

Key words: transmembrane 6 superfamily member, hepatocellular carcinoma, RNA sequencing, apoptosis, p53 signaling pathway

Introduction

Hepatocellular carcinoma (HCC) is the most common pathological type of primary liver cancer, is the third leading cause of cancer-associated death worldwide and is associated with a high metastatic potential and a high mortality rate (1). China, as one of the high-risk regions for liver cancer, is estimated to have approximately half of all liver cancer cases and mortalities (2). Although there are various treatments for HCC, including surgical resection, tumor ablation, radioembolization and molecular targeted therapy, the prognosis of patients with HCC remains poor (3). Recently, various molecular signatures, including a novel disulfidptosis-related immune checkpoint gene signature, have been developed to improve HCC prognosis prediction (4). Therefore, elucidating the mechanism of HCC development and identifying specific molecular biomarkers of HCC are important for effective HCC treatment and improving the prognosis of hepatocellular carcinoma.

The transmembrane 6 superfamily member 2 (TM6SF2) gene was first reported in 2000. It is located on the short arm of chromosome 19, encodes a protein consisting of 351 amino acids with a size of ~39.5 KDa, and is expressed primarily in specific organs of the body, such as the liver, small intestine, and kidney (5,6). The TM6SF2 gene is highly expressed in normal liver tissue, and the encoded protein is associated with triglyceride (TG) content in the liver and total cholesterol content in plasma is closely related (7). When expression of

the TM6SF2 gene is suppressed, TG content in hepatocytes increases, and the size and number of lipid droplets in the liver increase, which can cause liver injury (8,9). Several studies on TM6SF2 have focused on the rs58542926 variant, which has been shown to be closely associated with the development of non-alcoholic fatty liver disease (NAFLD) (10-12). This gene variant can additionally lead to an increased susceptibility to HCC (13).

At present, only a limited number of studies have investigated the role of TM6SF2 in HCC. In conjunction with the results of a previous study (14), functional experiments were conducted to further elucidate the role of TM6SF2 in HCC cells. In addition, the gene expression profile of TM6SF2-overexpressing HCC cells has not been fully investigated. Therefore, in the present study, TM6SF2 expression in HCC was examined, and its biological effects in Huh-7 cells were evaluated. RNA sequencing (RNA-Seq), Gene Ontology (GO) enrichment analysis, and Kyoto Encyclopedia of Genes and Genomes (KEGG) pathway analysis were performed to explore the potential molecular mechanisms underlying the effects of TM6SF2 in HCC cells.

Materials and methods

Public data acquisition and bioinformatics analysis. The RNA-Seq mRNA expression profile of TM6SF2 in Liver Hepatocellular Carcinoma (LIHC) was obtained from The Cancer Genome Atlas (TCGA) Genomic Data Commons (GDC) data portal (https://portal.gdc.cancer.gov/); it consists of data on 374 LIHC and 50 adjacent normal tissues, along with the corresponding clinical data. Patients with insufficient clinical and expression information were excluded. The 5-year survival curve for patients, based on median TM6SF2 expression, was analyzed using the Kaplan-Meier Plotter. Additional TCGA-based analyses were performed using publicly available TCGA-LIHC data obtained from UCSC Xena (https://xenabrowser.net/datapages/). TM6SF2 expression data, clinical information, survival data and somatic mutation data were downloaded and integrated according to TCGA sample identifiers. Patients with incomplete survival or clinical information were excluded from the corresponding analyses. Patients were divided into high- and low-TM6SF2 expression groups according to the median expression value. Univariate and multivariate Cox regression analyses were performed to evaluate the association between TM6SF2 expression and overall survival, together with available clinical variables, including age, sex and pathological stage. The association between TM6SF2 expression and clinicopathological features was assessed using the Mann-Whitney U test or Spearman's correlation analysis, as appropriate. TP53 mutation status was determined from the somatic mutation data, and TM6SF2 expression was compared between TP53-mutant and TP53-wild-type samples.

Cell culture and lentiviral transfection. The human hepatoma cell line Huh-7 (Procell Life Science & Technology Co., Ltd.) was cultured in DMEM (cat. no. PM150210; Procell Life Science & Technology Co., Ltd.) with 10% FBS (cat. no. 10099141C; Gibco; Thermo Fisher Scientific, Inc.) and 1% Penicillin-Streptomycin (10,000 U/ml; cat. no. 15140122; Invitrogen; Thermo Fisher Scientific, Inc.) at 37˚C in a 5% CO_2 humidified incubator. The TM6SF2 overexpression lentivirus and the corresponding empty vector control lentivirus were constructed and packaged by GeneCopoeia, Inc. using a third-generation lentiviral packaging system. Briefly, lentiviral particles were produced in 293T cells obtained from Jiangsu KeyGen Biotech Co., Ltd. by co-transfection of the lentiviral expression plasmid, packaging plasmid and envelope plasmid at a mass ratio of 4:3:1. The amount of lentiviral expression plasmid used for packaging was 10 μg. Lentiviral particles were collected at 48 and 72 h after transfection. Huh-7 cells were infected with the TM6SF2 overexpression lentivirus or empty vector control lentivirus at a multiplicity of infection of 10 in the presence of polybrene. At 12 h after infection, the culture medium containing lentiviral particles was replaced with fresh complete medium. At 96 h after infection, cells were selected with puromycin at 1 μg/ml. The medium was replaced every 2 days, and cells were cultured for 2 weeks to obtain stable cell lines. Stable cells were maintained in medium containing 0.5 μg/ml puromycin.

Reverse transcription-quantitative (RT-q) PCR. Total RNA was extracted from Huh-7 cells seeded at a density of $2x10^5$ cells/well in six-well plates using RNA Isolator Total RNA Extraction Reagent (cat. no. R401-01; Vazyme Biotech Co., Ltd.) according to the manufacturer's protocol. The cDNA was reverse transcribed using Hiscript III Reverse Transcriptase (cat. no. R302-01; Vazyme Biotech Co., Ltd.) according to the manufacturer's protocol. Quantitative PCR was performed using Taq Pro Universal SYBR qPCR Master Mix (cat. no. Q712-02; Vazyme Biotech Co., Ltd.) on a LightCycler 96SW1.1 real-time PCR system (Roche Diagnostics GmbH). The qPCR cycling conditions were: Initial denaturation at 95˚C for 5 min, followed by 40 cycles of denaturation at 95˚C for 10 sec and annealing/extension at 60˚C for 30 sec. Melting curve analysis was performed at 95˚C for 15 sec, 60˚C for 60 sec and 95˚C for 15 sec. GAPDH was selected as the internal reference to evaluate the efficiency of TM6SF2 overexpression. The primer sequences are listed in Table I. The expression levels of DEGs in different groups were normalized to GAPDH mRNA levels using the $2^{-\Delta\Delta Cq}$ method (15). Each sample was analyzed in triplicate and all RT-qPCR experiments were repeated three times.

Western blotting. Protein samples were extracted using RIPA lysis buffer containing protease and phosphatase inhibitors (Beyotime Biotechnology). Total protein content was measured using a BCA kit (Beyotime Biotechnology) according to the manufacturer's protocol. Equal amounts of protein (30 μg/lane) were separated by SDS-PAGE on 10% gels and transferred onto PVDF membranes. The membranes were blocked with 5% skimmed milk at room temperature for 2 h. Membranes were incubated with primary antibodies against TM6SF2 (cat. no. A18649; ABclonal Biotech Co., Ltd.), p53 (cat. no. A25915; ABclonal Biotech Co., Ltd.), phosphorylated p53 (cat. no. AP0986; ABclonal Biotech Co., Ltd.), p21 (cat. no. A19094; ABclonal Biotech Co., Ltd.), Cyclin E1 (cat. no. A22360; ABclonal Biotech Co., Ltd.), PERP (cat. no. A5937; ABclonal Biotech Co., Ltd.), FAS (cat. no. A19582; ABclonal Biotech Co., Ltd.), PUMA

Table I. Primer sequences for reverse transcription-quantitative PCR.

Gene name	Forward primer sequence (5'-3')	Reverse primer sequence (5'-3')
GAPDH	AACGGATTTGGTCGTATTG	GGAAGATGGTGATGGGATT
TM6SF2	CTTCGTGTGCAATCTGCTGTAT	CAATGCTGCTTCTTGTGGCG
IGFBP3	AGAGCACAGATACCCAGAACT	GGTGATTCAGTGTGTCTTCCATT
CDK6	CCAGATGGCTCTAACCTCAGT	AACTTCCACGAAAAAGAGGCTT
ATM	ATCTGCTGCCGTCAACTAGAA	GATCTCGAATCAGGCGCTTAAA
ATR	GGCCAAAGGCAGTTGTATTGA	GTGAGTACCCCAAAAATAGCAGG
PTEN	TGGATTCGACTTAGACTTGACCT	GGTGGGTTATGGTCTTCAAAAGG
TP53	CAGCACATGACGGAGGTTGT	TCATCCAAATACTCCACACGC
CYCS	CTTTGGGCGGAAGACAGGTC	TTATTGGCGGCTGTGTAAGAG
TSP1	AGACTCCGCATCGCAAAGG	TCACCACGTTGTTGTCAAGGG
CCNB2	CCGACGGTGTCCAGTGATTT	TGTTGTTTTGGTGGGTTGAACT
GADD45B	TACGAGTCGGCCAAGTTGATG	GGATGAGCGTGAAGTGGATTT
TGFBR1	ACGGCGTTACAGTGTTTCTG	GCACATACAAACGGCCTATCTC
PERP	CTTCACCCTTCATGCCAACC	GCCAATCAGGATAATCGTGGCT
CCNE1	GCCAGCCTTGGGACAATAATG	CTTGCACGTTGAGTTTGGGT
DDB2	ACCTCCGAGATTGTATTACGCC	TCACATCTTCTGCTAGGACCG
FAS	TCTGGTTCTTACGTCTGTTGC	CTGTGCAGTCCCTAGCTTTCC
CD82	TGTCCTGCAAACCTCCTCCA	CCATGAGCATAGTGACTGCCC
BBC3	GACCTCAACGCACAGTACGAG	AGGAGTCCCATGATGAGATTGT
CDKN1A	TGTCCGTCAGAACCCATGC	AAAGTCGAAGTTCCATCGCTC
TGFBI	GGCCAGATCCTGTCCAAGC	GTGGGTTTCCACCATTAGCAC
PER1	GCCAACCAGGAATACTACCAGC	GTGTGTACTCAGACGTGATGTG

(cat. no. A3752; ABclonal Biotech Co., Ltd.), cytochrome c (cat. no. A4912; ABclonal Biotech Co., Ltd.) and β-actin (cat. no. AC026; ABclonal Biotech Co., Ltd.) overnight at 4˚C. β-actin was used as the reference protein. The primary antibodies were diluted at 1:1,000. After washing three times with TBST for 10 min each, the membranes were incubated with HRP-conjugated goat anti-rabbit IgG secondary antibody (cat. no. AS014; ABclonal Biotech Co., Ltd.) at a dilution of 1:5,000 at room temperature for 2 h. Signals were visualized with SuperSignal West Pico PLUS chemiluminescence solution (Thermo Fisher Scientific, Inc.) and imaged using a Bio-Rad ChemiDoc XRS+ imaging system (Bio-Rad Laboratories, Inc.). Densitometric analysis was performed using ImageJ software version 1.53 (National Institutes of Health).

Detection of cell proliferation. A Cell Counting Kit 8 (CCK-8) assay (cat. no. C0038; Beyotime Biotechnology) was used to detect cell viability. In different groups, $2x10^3$ cells (100 μl) were added to each well in a 96-well plate. A total of 5 identical plates were plated to assess cell proliferation at 0, 24, 48, 72 and 96 h. At the corresponding detection point, 10 μl CCK-8 solution was added to each well, and the cells were incubated for another 2 h, after which the absorbance was measured at 450 nm.

For colony formation assays, cells were collected. A total of 700 cells were plated per well in six-well plates, with 3 replicate wells prepared for each cell group. The plates were cultured until visible colonies appeared, after which the cultures were terminated. Colonies were defined as cell clusters containing >50 cells. Subsequently, the supernatant was discarded, and cells were fixed with 4% paraformaldehyde at room temperature for 20 min, stained with crystal violet at room temperature for 15 min, and images were captured. The number of colonies formed was quantified using ImageJ software version 1.53 (National Institutes of Health).

Wound healing assay. Huh-7 cells from the TM6SF2 and Vector groups were seeded into six-well plates at a density of 8x10^5 cells/well and cultured until a confluent monolayer formed. A straight scratch was made using a sterile 200-μl pipette tip. Detached cells were removed by washing with PBS, and the cells were then cultured in serum-free DMEM. Images were captured at 0 and 24 h using an inverted light microscope. Wound closure was quantified using ImageJ software version 1.53 (National Institutes of Health) by measuring the wound width at 0 and 24 h, and the migration rate was calculated relative to the initial wound width.

Transwell assay. For the Transwell migration assay, cells were serum starved for 24 h, 200 μl of the cell suspension (density $4x10^5$ cells /ml) was added to the upper chamber of the Transwell insert (Guangzhou Jet Bio-Filtration Co., Ltd.) and 600 μl supplemented DMEM (15% FBS) was added to the lower chamber. After 24 h of culture, the Transwell chamber was removed and cells were fixed with 4% paraformaldehyde at room temperature for 20 min and stained with crystal violet at room temperature for 15 min. Cells that did not cross the upper surface of the permeable membrane were gently wiped off. A

total of five fields of view were selected for each chamber, and cell counts were performed using an inverted microscope. The experiment was repeated three times for each group of cells.

For the Transwell invasion assay, the Transwell inserts were coated with Matrigel (BD Biosciences) diluted 1:10 by evenly layering it on the permeable membrane of the Transwell insert, then left to solidify by incubating at 37˚C for 4 h. The starved cell suspension was added to the upper chamber of the Transwell insert, and supplemented DMEM (15% FBS) was added to the lower chamber as per the migration assay. All other experimental procedures were the same as the Transwell migration assay.

Flow cytometry analysis. To assess apoptosis, cells were cultured in six-well plates. After cells reached ~85% confluence, they were collected and stained with an Annexin V-PE/7-AAD double staining apoptosis assay kit according to the manufacturer's protocol (Jiangsu KeyGen Biotech Co., Ltd.). Briefly, cells were resuspended in binding buffer and stained with Annexin V-PE and 7-AAD at room temperature for 10 min in the dark. The apoptotic rate was calculated as the percentage of early apoptotic cells plus late apoptotic cells, defined as Annexin V-PE-positive/7-AAD-negative cells plus Annexin V-PE-positive/7-AAD-positive cells. For cell cycle analysis, cells were stained using the Cell Cycle and Apoptosis Analysis Kit (Beyotime Biotechnology) according to the manufacturer's protocol. Briefly, cells were fixed in 70% ethanol at 4˚C overnight and then stained with PI/RNase A staining solution at 37˚C for 30 min in the dark. The samples were immediately analyzed using a BD FACSCanto flow cytometer (BD Biosciences). Data were analyzed using FlowJo software version 10.8.1 (BD Biosciences). All experiments were repeated in triplicate.

RNA-Seq. RNA samples from the TM6SF2 and control Vector groups were sequenced with three replicates per group at Novogene Co., Ltd. RNA was extracted from cells using TRIzol® (Invitrogen; Thermo Fisher Scientific, Inc.), followed by rigorous quality control using an RNA Nano 6000 Assay Kit on a Bioanalyzer 2100 system (Agilent Technologies, Inc.). The RNA library was constructed using NEBNext Ultra Directional RNA Library Prep Kit for Illumina (New England BioLabs, Inc.). The insert size of the acquired library was checked using an Agilent 2100 Bioanalyzer (Agilent Technologies, Inc.). After library preparation, the samples were sequenced on the Illumina NovaSeq 6000 platform (Illumina, Inc.) by Novogene Co., Ltd., yielding 150-bp paired-end reads. The paired-end clean reads were aligned to the human reference genome using the software HISAT2 (16). The RNA-Seq data files have been deposited in the Sequence Read Archive under BioProject accession no. PRJNA858660 (https://www.ncbi.nlm.nih.gov/bioproject/PRJNA858660).

Screening of DEGs. After processing and analysis of RNA-Seq data, the alignment results were transferred to StringTie v2.1.7 (https://ccb.jhu.edu/software/stringtie/) for transcript assembly (17). Gene expression levels are reported as Fragments per kilobase of transcript sequence per million base pairs sequenced (FPKM). The DEGs between the TM6SF2 group and the Vector group were identified using DESeq2 v1.36.0 (https://bioconductor.org/packages/release/bioc/html/DESeq2.html) in R v4.2.1 (https://www.r-project.org/). The resulting P-values were adjusted using Benjamini and Hochberg's approach for controlling the false discovery rate. Based on the DESeq2 method (18), genes with |log2 fold change|>0 and adjusted P<0.05 were considered DEGs. Functional enrichment analysis. GO and KEGG pathway enrichment analyses were performed for all DEGs, upregulated DEGs and downregulated DEGs. For the enrichment analyses of upregulated and downregulated genes, all DEGs were used as the background gene set. Therefore, due to differences in the background gene sets and enrichment calculations, some GO terms could be identified in the enrichment analysis of upregulated and downregulated genes but not in analyses performed using only isolated upregulated or downregulated gene subsets. GO terms and KEGG pathways with adjusted P<0.05 were considered significantly enriched.

Statistical analysis. All statistical analyses were performed using R version 4.2.1. All experiments were repeated three times, and data are presented as the mean ± standard deviation. Differences between two groups were analyzed using an independent samples t-test or paired t-test, as appropriate. For comparisons among more than two groups, one-way analysis of variance (ANOVA) followed by Tukey's post hoc multiple comparisons test was used. The correlation between RNA-Seq and RT-qPCR log2 fold-change values was assessed using Pearson's correlation analysis. The relationship between TM6SF2 expression and clinical characteristics was assessed using a Wilcoxon test. P<0.05 was considered to indicate a statistically significant difference.

Results

Low TM6SF2 expression is associated with poorer survival. TCGA data were used to analyze TM6SF2 mRNA expression in HCC tissues. TM6SF2 expression was found to be downregulated in HCC tissues compared with unpaired normal tissues (Fig. 1A) or paired adjacent normal tissues (Fig. 1B). The relationship between TM6SF2 expression and clinicopathological parameters showed that TM6SF2 expression was negatively associated with tumor stage (Fig. 1C). The 5-year survival curve of patients with HCC stratified by TM6SF2 expression was analyzed using KM-Plotter. The 5-year survival rate of patients with low TM6SF2 expression was significantly lower than those with high expression (Fig. 1D). Together, these results suggested that TM6SF2 expression was preliminarily associated with survival and tumor stage in the analyzed TCGA-LIHC cohort. To further evaluate the clinical relevance of TM6SF2 expression in HCC, additional TCGA-based analyses were performed. Univariate and multivariate Cox regression analyses were conducted using available clinical variables, including age, sex and pathological stage. In the multivariate Cox regression model, pathological stage remained significantly associated with overall survival, whereas TM6SF2 expression was not identified as an independent prognostic factor (Table SI). Additional clinicopathological correlation analyses showed that TM6SF2 expression was weakly negatively correlated with pathological stage (Table SII). Furthermore, TM6SF2 expression tended

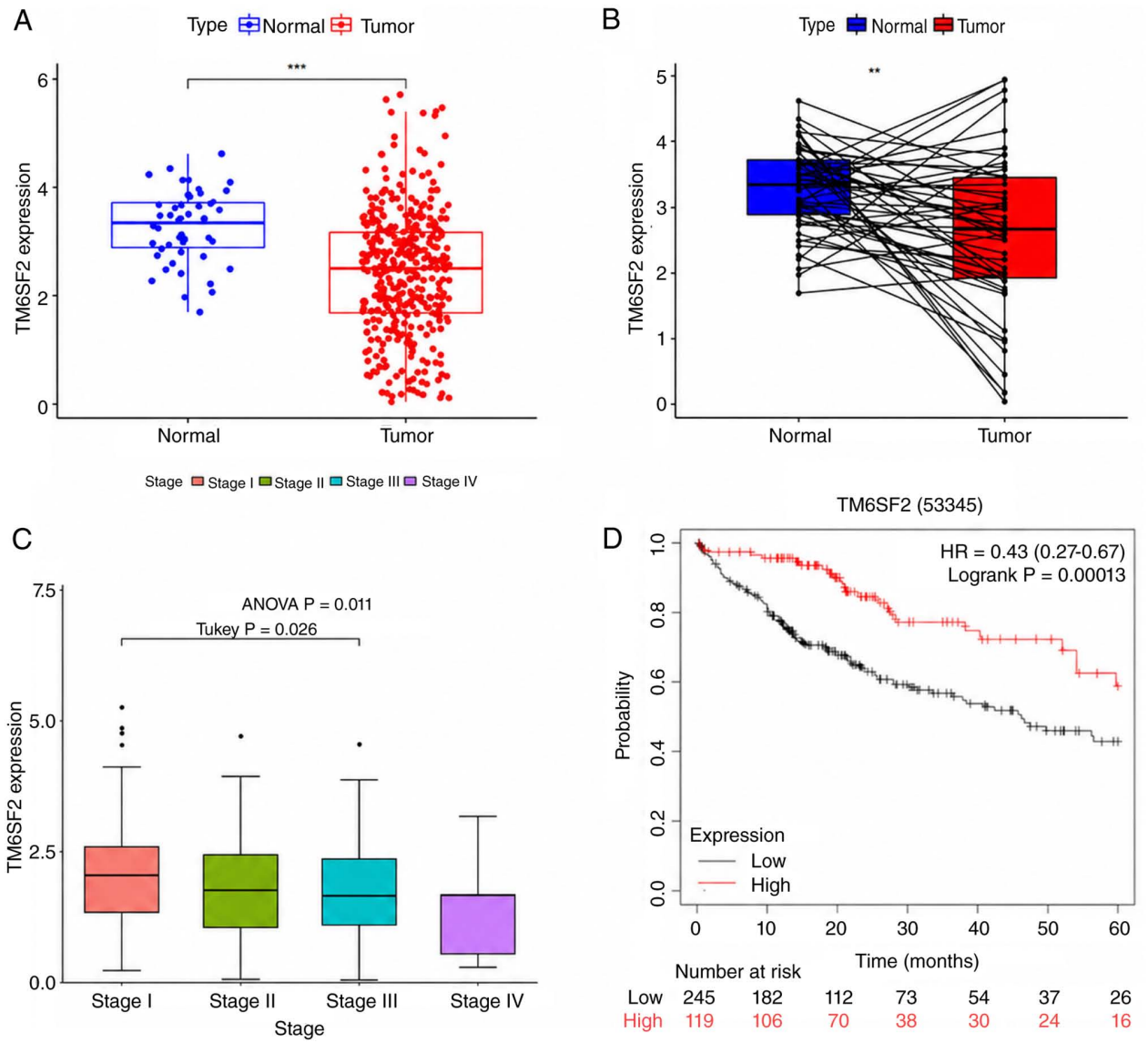

Figure 1. The results of bioinformatics analysis of TM6SF2 in HCC. (A) Differential expression of TM6SF2 in HCC and normal liver tissues. (B) Differential expression of TM6SF2 in paraneoplastic tissues and paired HCC tissues. (C) Correlation between TM6SF2 expression and tumor stage. (D) 5-year survival curve of patients with HCC based on TM6SF2 expression. TM6SF2, transmembrane protein 6 superfamily member 2; HCC, hepatocellular carcinoma. **P<0.01 and ***P<0.001.

to be lower in TP53-mutant samples than in TP53-wild-type samples, although the difference did not reach statistical significance (Fig. S1). These results suggested that TM6SF2 expression is associated with certain clinical features in the analyzed TCGA-LIHC cohort; however, its independent prognostic value requires further validation.

TM6SF2 inhibits the proliferation of Huh-7 hepatoma cells. To evaluate the effect of TM6SF2 on cell growth, TM6SF2 was overexpressed in Huh-7 cells. Western blotting and RT-qPCR confirmed the results. The results showed that TM6SF2 was effectively overexpressed in Huh-7 cells (Fig. 2A and B).

The effect of TM6SF2 overexpression on cell growth was assessed using CCK-8 and colony formation assays. Compared with the control Vector group, TM6SF2 overexpression significantly reduced cell viability (Fig. 2C; P<0.05). Additionally, the number of colonies formed in the TM6SF2 group was reduced compared with the control Vector group (Fig. 2D, P<0.05). Taken together, these results indicated that TM6SF2 inhibited the proliferation and colony formation of Huh-7 cells.

TM6SF2 reduces the metastatic ability of Huh-7 hepatoma cells. In wound healing and Transwell migration assays, the migratory ability of Huh-7 cells in the TM6SF2 group was significantly decreased compared with the control Vector group (Fig. 3A and B; P<0.05). The results of the Transwell invasion assay showed that, compared with the control Vector group, Huh-7 cell invasion in the TM6SF2 overexpression group was significantly reduced (Fig. 3C, P<0.05).

TM6SF2 induces S-phase cell-cycle arrest and apoptosis. To further investigate the inhibitory mechanism of TM6SF2 in Huh-7 cells, flow cytometry was used to assess whether its

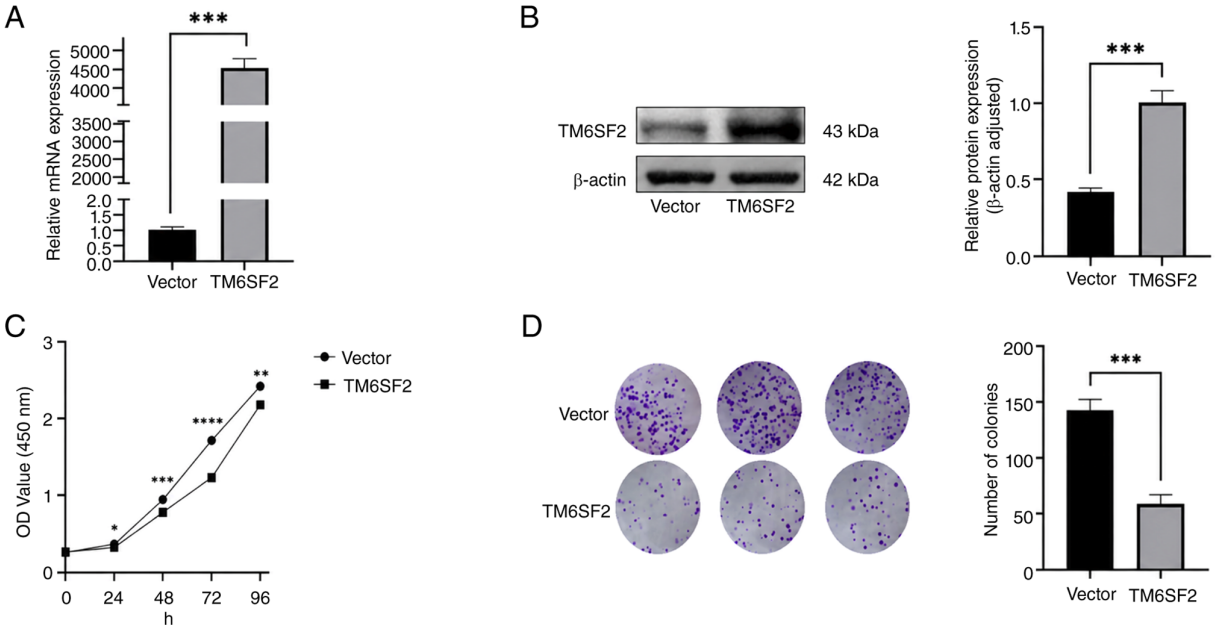

Figure 2. Overexpression of TM6SF2 inhibits the proliferation of Huh-7 human HCC cells. (A and B) Evaluation of the efficiency of TM6SF2 overexpression in Huh-7 cells. (C) CCK-8 assays were used to assess the proliferative ability of Huh-7 cells in the TM6SF2 and control Vector groups. (D) Colony formation assays were used to detect the proliferation of Huh-7 cells in the TM6SF2 and control Vector groups. *P<0.05, **P<0.01, ***P<0.001 and ****P<0.0001 vs. Vector group. TM6SF2, transmembrane protein 6 superfamily member 2; HCC, hepatocellular carcinoma.

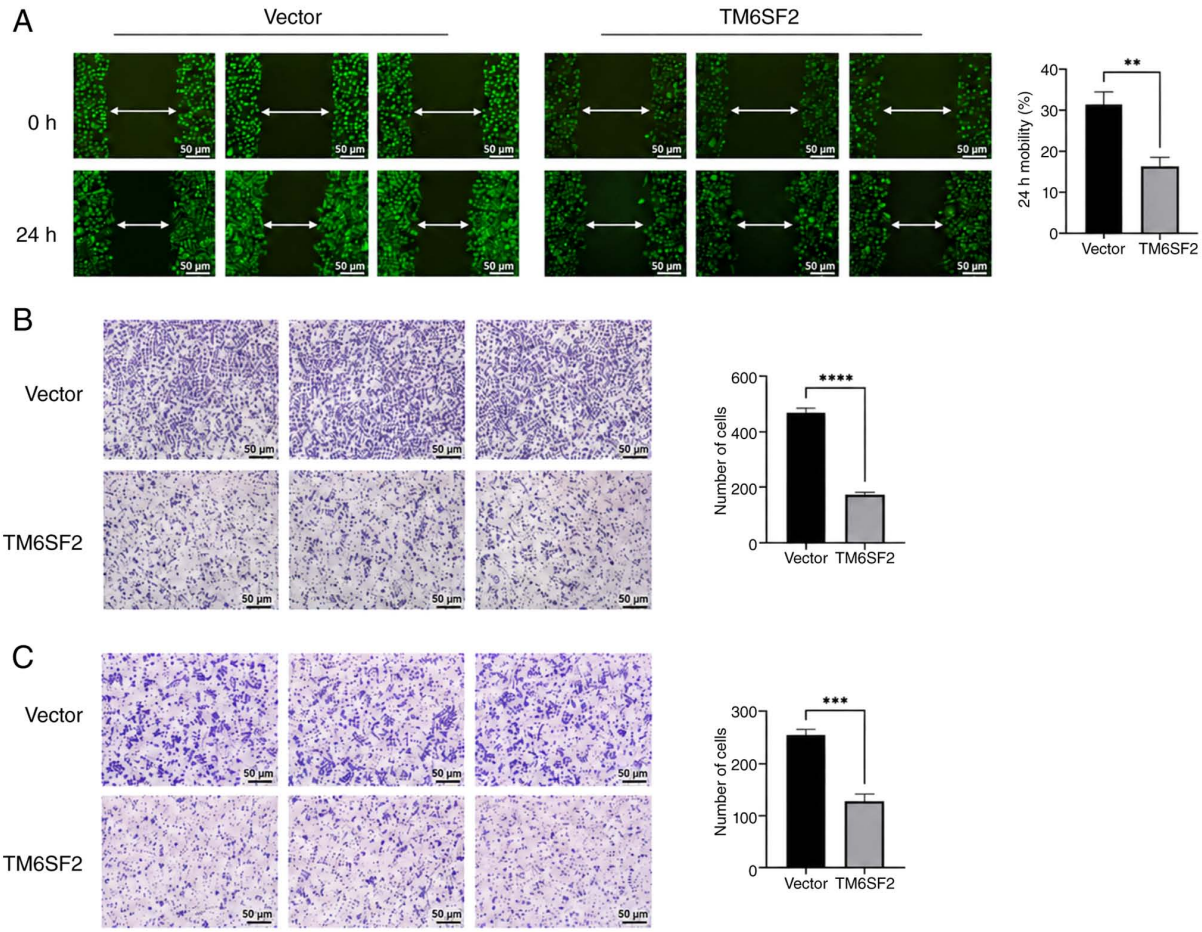

Figure 3. Overexpression of TM6SF2 inhibits metastasis of Huh-7 human HCC cells. (A and B) The migratory ability of Huh-7 cells in the TM6SF2 and control Vector groups was assessed using wound-healing and Transwell assays. The wound width measured in the wound-healing assay is indicated by white double-headed arrows. (C) The invasive ability of Huh-7 cells in the TM6SF2 and control Vector groups was assessed using Transwell assays. Images in panels A-C were captured at x100 magnification. Scale bars, 50 μm. **P<0.01, ***P<0.001 and ****P<0.0001 vs. Vector group. TM6SF2, transmembrane protein 6 superfamily member 2; HCC, hepatocellular carcinoma.

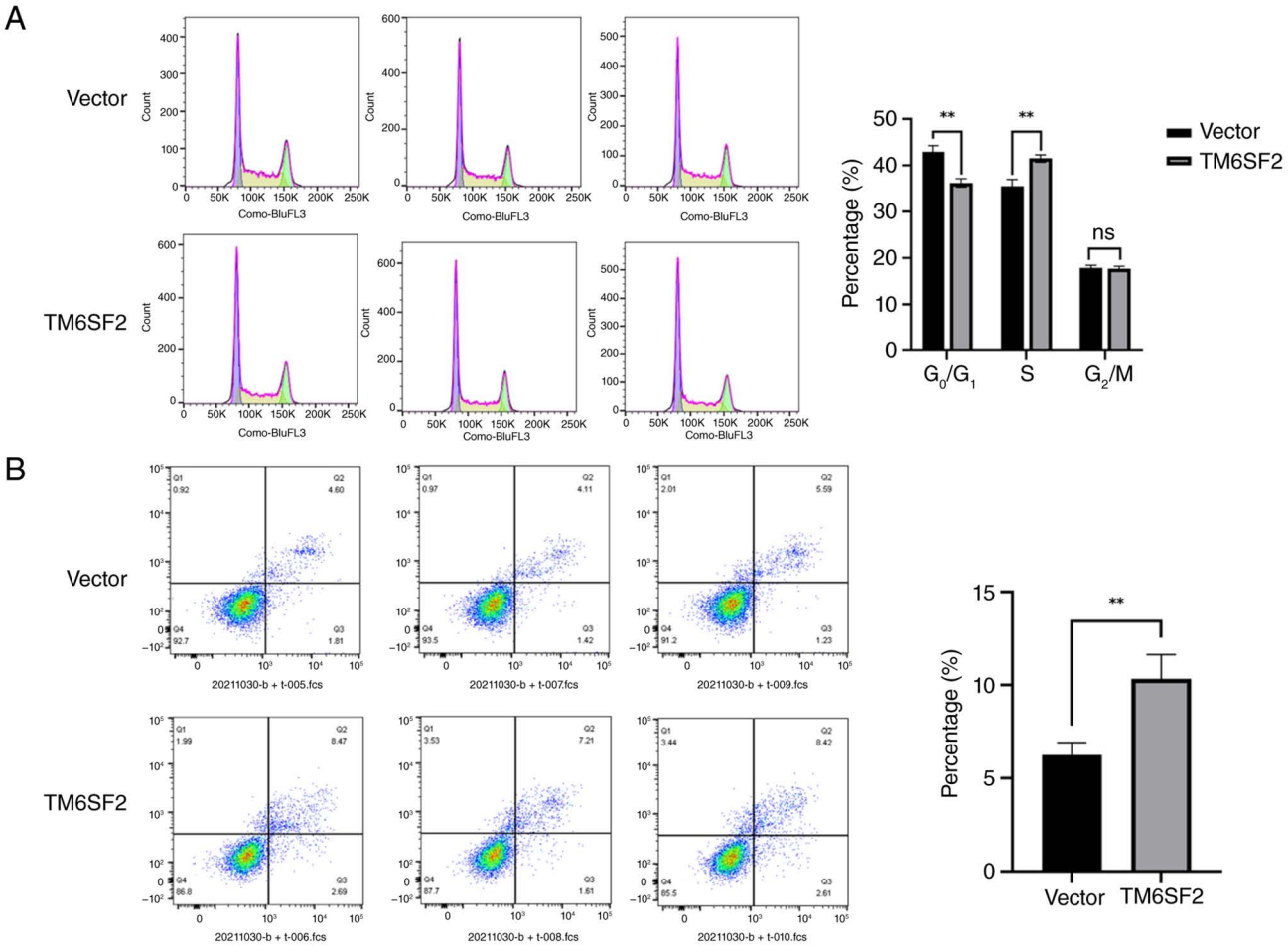

Figure 4. TM6SF2 overexpression induces S-phase cell-cycle arrest and apoptosis in Huh-7 cells. (A) Effect of TM6SF2 overexpression on cell-cycle distribution. (B) Effect of TM6SF2 overexpression on apoptosis in Huh-7 cells. TM6SF2, transmembrane protein 6 superfamily member 2. **P<0.01 vs. Vector group; ns, not significant.

antiproliferative effect was mediated by cell cycle arrest. As shown in Fig. 4A, compared with the control Vector group, the number of cells in the S phase of the TM6SF2 group significantly increased, the number of cells in the G_1 phase decreased, and the number of cells in the G2/M phase did not change. This highlighted the role of TM6SF2 in regulating the cell cycle in Huh-7 cells. These results indicated that TM6SF2 overexpression induced S-phase cell-cycle arrest in Huh-7 cells. The decrease in the proportion of cells in the G_1 phase may reflect an accumulation of cells in S phase rather than an acceleration of the G_1/S transition. In addition, compared with the control Vector group, the number of apoptotic cells in Huh-7 was significantly increased in the TM6SF2 group (Fig. 4B).

TM6SF2 overexpression alters the gene expression profile of Huh-7 cells. To investigate the role of TM6SF2 in human HCC cells, RNA-Seq was performed on TM6SF2-overexpressing Huh-7 cells and control Huh-7 cells (control Vector group) (PRJNA858660). FPKM was used to represent gene expression levels from RNA-Seq data. A total of three biological replicates were performed for each group, and the results showed a significant association between the TM6SF2 group and the Vector group (Fig. 5A). Taking the $|\log_2$ (Fold Change)|>0 and P-adj<0.05 as the criteria for the classification of DEGs, there were a total of 3,071 DEGs induced by TM6SF2 overexpression, including 1,571 upregulated genes and 1,500 downregulated genes (Fig. 5B). The list of DEGs is provided in Table SIII. To validate the DEGs identified by RNA-Seq, the expression levels of 20 screened differential genes were quantified by RT-qPCR. Between the two techniques, the Pearson correlation coefficient for fold changes in gene expression levels was 0.82 (P<0.001; Fig. 5C).

Overview of the effects of TM6SF2 overexpression on the biological functions of Huh-7 cells. To explore the potential biological functions of TM6SF2-related genes, GO and KEGG analyses were performed using the significant DEGs. The GO biological processes enriched in the up- and downregulated genes were primarily related to cell growth, regulation of cell growth and negative regulation of growth (Fig. 6A); the complete list of processes is listed in Table SIV. The enriched GO terms for the upregulated and downregulated DEG subsets are shown in Fig. 6B and C and listed in Tables SV and SVI.

With TM6SF2 overexpression, only two KEGG pathways with P-adj<0.05 were identified: the p53 signaling pathway and Small cell lung cancer (Fig. 6D; Table SVII). Since <20 enriched KEGG pathways reached significant levels after

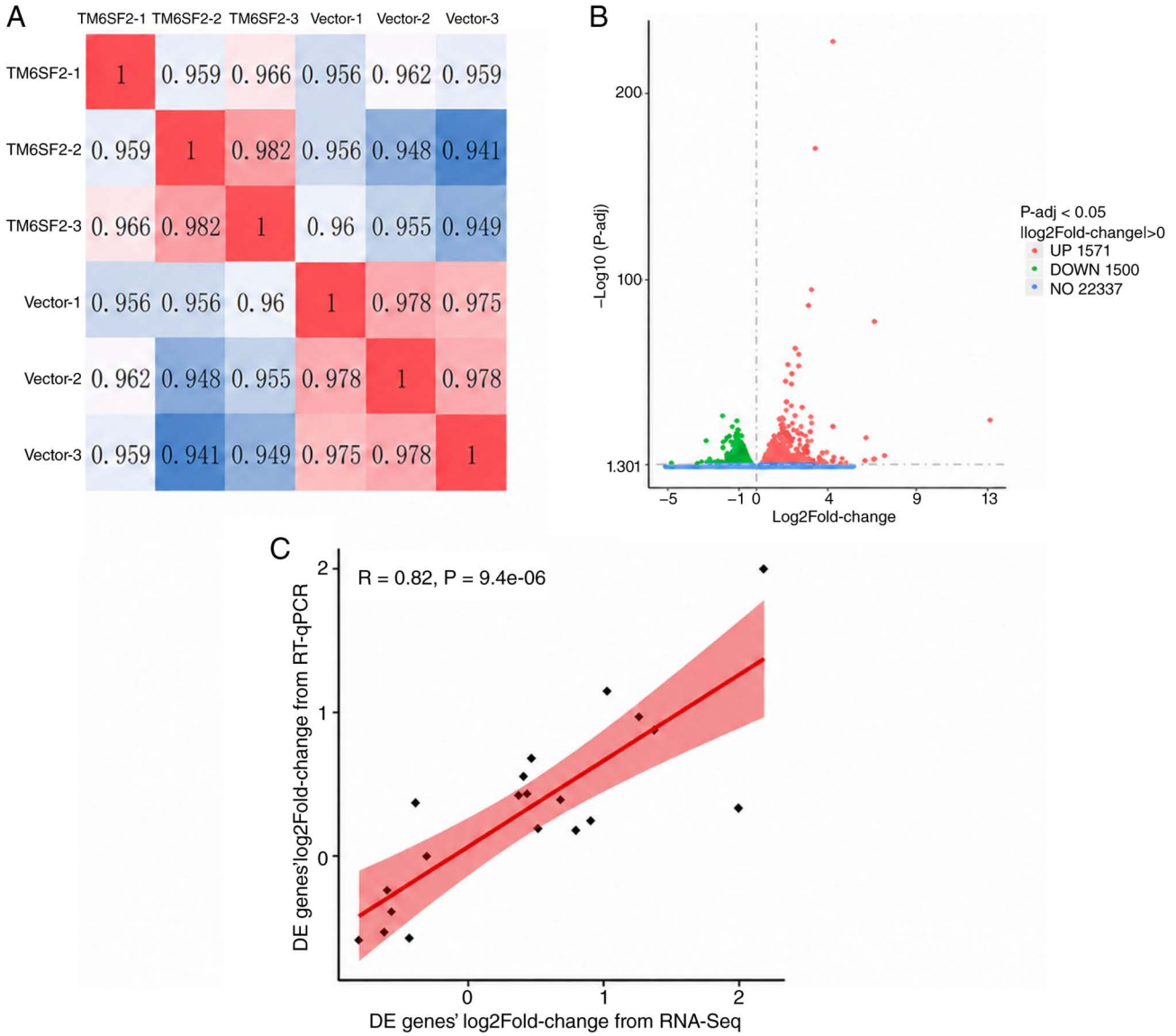

Figure 5. TM6SF2 overexpression alters the gene expression profile of Huh-7 cells. (A) Correlation analysis of RNA-Seq samples from the TM6SF2 overexpression group and the control Vector group, with three biological replicates in each group. (B) Volcano plot showing differentially expressed genes between the TM6SF2 group and the Vector group. (C) Correlation between $\log_2$ fold-change values obtained from RNA-Seq and RT-qPCR validation for selected significant DEGs. The correlation coefficient shown in panel C is Pearson's r. TM6SF2, transmembrane protein 6 superfamily member 2; RNA-Seq, RNA sequencing; RT-qPCR, reverse transcription-quantitative PCR; DEG, differentially expressed gene.

adjustment for P-values, Fig. 6D lists the top 20 most enriched KEGG pathways across all DEGs according to P-values.

TM6SF2 overexpression is associated with p53-related molecular changes in Huh-7 cells. RNA-Seq results indicated that genes altered by TM6SF2 overexpression were enriched in the p53 signaling pathway, suggesting that p53-related molecular changes may be associated with TM6SF2 overexpression. A total of 27 DEGs between the TM6SF2 and control Vector groups were involved in the p53 signaling pathway, including 16 upregulated genes and 11 downregulated genes. In the KEGG-enriched p53 signaling pathway diagram, red and green boxes represent upregulated and downregulated genes, respectively (Fig. 7). As a tumor suppressor protein, p53 regulates genes involved in cell-cycle control, apoptosis, DNA damage response, and other biological processes. After TM6SF2 overexpression, phosphorylated p53 was increased, indicating p53-related post-translational molecular changes. Consistently, molecular validation showed that several genes involved in these processes were altered at the mRNA or protein levels (Fig. 8).

Discussion

Hepatocarcinogenesis is a multifactorial, multistage process with complex pathogenesis involving abnormal expression of several genes. The discovery of genes causally linked to hepatocarcinoma and the identification of novel therapeutic targets informed by their mechanisms of action, represent important areas of tumor biology research (19). Beyond its role in cancer, the liver is a central organ for secreting vital enzymes. For example, research on transgenic mouse milk expressing human bile salt-stimulated lipase has shown that such liver-related proteins can improve the survival and

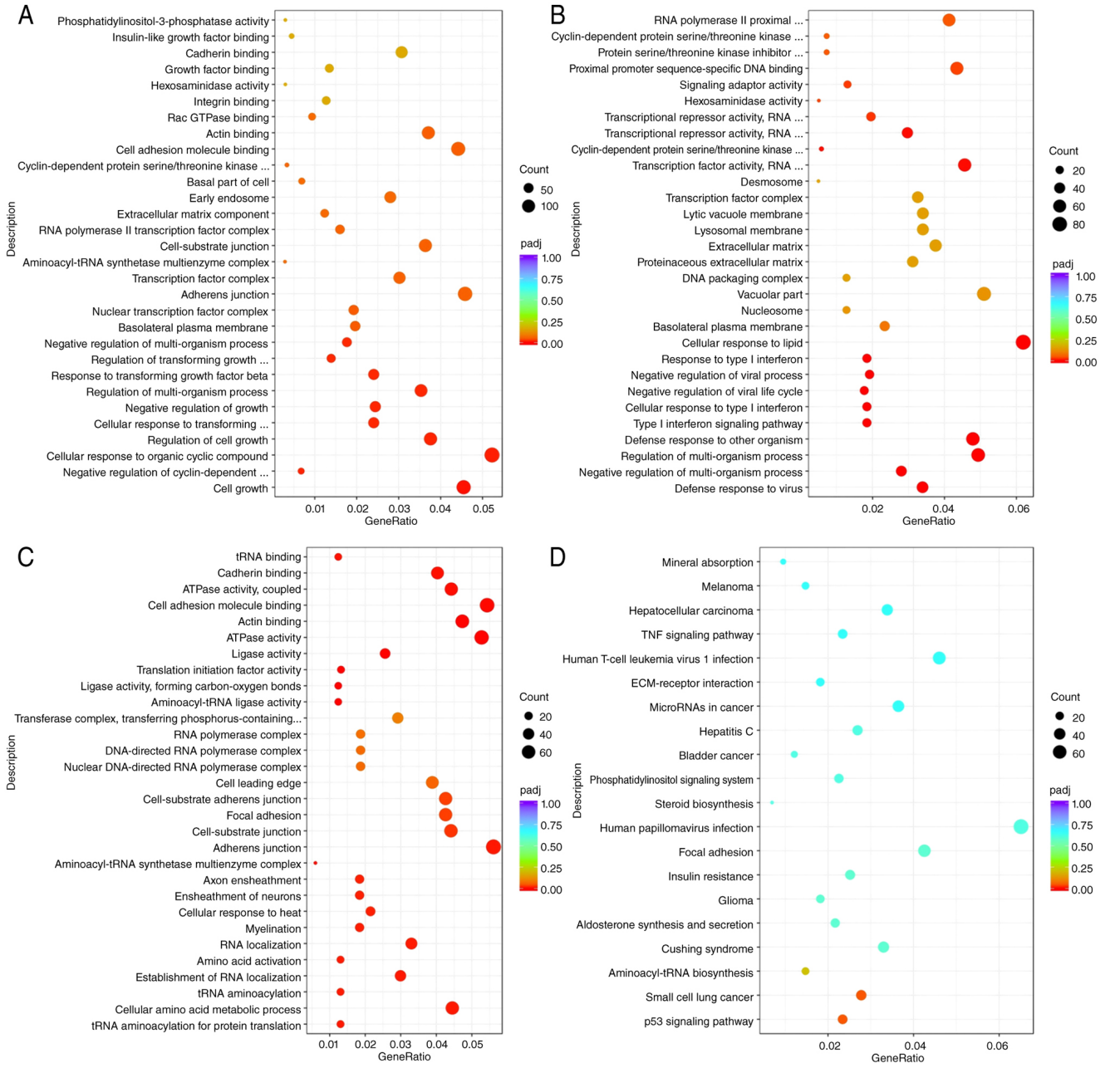

Figure 6. Potential biological functions of TM6SF2-associated genes in Huh-7 cells. (A) Top 30 GO terms in up- and downregulated DEGs. (B) Top 30 GO terms in up-regulated DEGs. (C) Top 30 GO terms in downregulated DEGs. (D) Top 20 most enriched KEGG pathways across all DEGs. TM6SF2, transmembrane protein 6 superfamily member 2; GO, Gene Ontology; DEG, differentially expressed gene.

growth of premature mice, emphasizing the diverse physiological importance of hepatic protein expression (20). In 2014, Kozlitina *et al* (7) first reported that polymorphisms at the rs58542926 (E167K) locus of the TM6SF2 gene were significantly associated with the occurrence of NAFLD. Subsequent studies have confirmed and refined the conclusion that the TM6SF2 E167K variant impairs normal TM6SF2 protein function, disrupting its role in lipid metabolism and thereby contributing to the development of NAFLD and cardiovascular disease (21-23).

The role of TM6SF2 in hepatocarcinoma development has only recently been investigated. Few studies have examined the mechanisms by which TM6SF2 contributes to hepatocarcinogenesis or the downstream regulatory pathways it modulates. Bioinformatics analyses and cell function experiments have shown that TM6SF2 is expressed at low levels in HCC tissues and that restoring or increasing its expression to above-normal levels may exert a tumor-suppressive effect. However, the genes and pathways involved in tumor suppression following TM6SF2 overexpression in HCC cells remain unclear. Therefore, transcriptome analysis of DEGs following TM6SF2 overexpression was performed using RNA-seq. In total, 3,071 DEGs were identified, including 1,571 upregulated and 1,500 downregulated genes. Cell-function experiments further confirmed that TM6SF2 overexpression significantly reduced HCC cell proliferation and colony-formation rates and effectively inhibited their metastatic potential, including migration and invasion. In addition, TM6SF2 overexpression

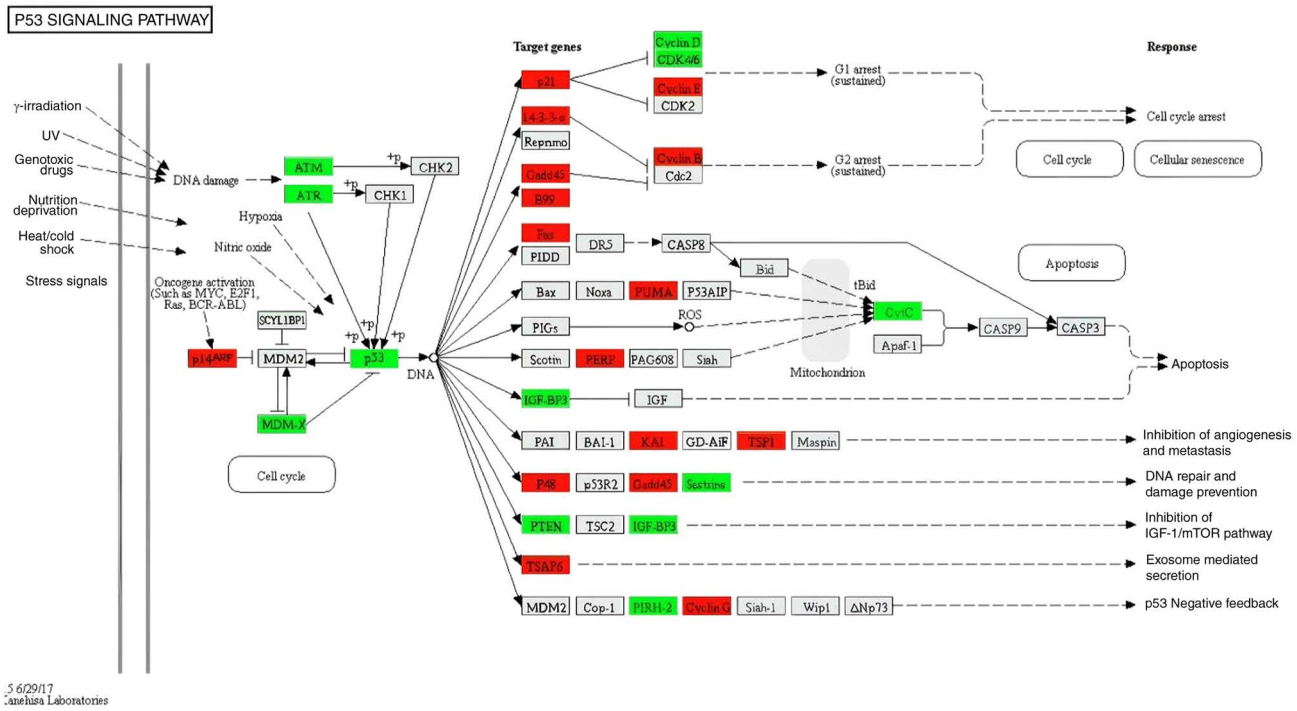

Figure 7. Kyoto Encyclopedia of Genes and Genomes diagram of the p53 signaling pathway. Red boxes indicate upregulated genes, green boxes indicate downregulated genes and white boxes indicate genes in the pathway that were not significantly differentially expressed.

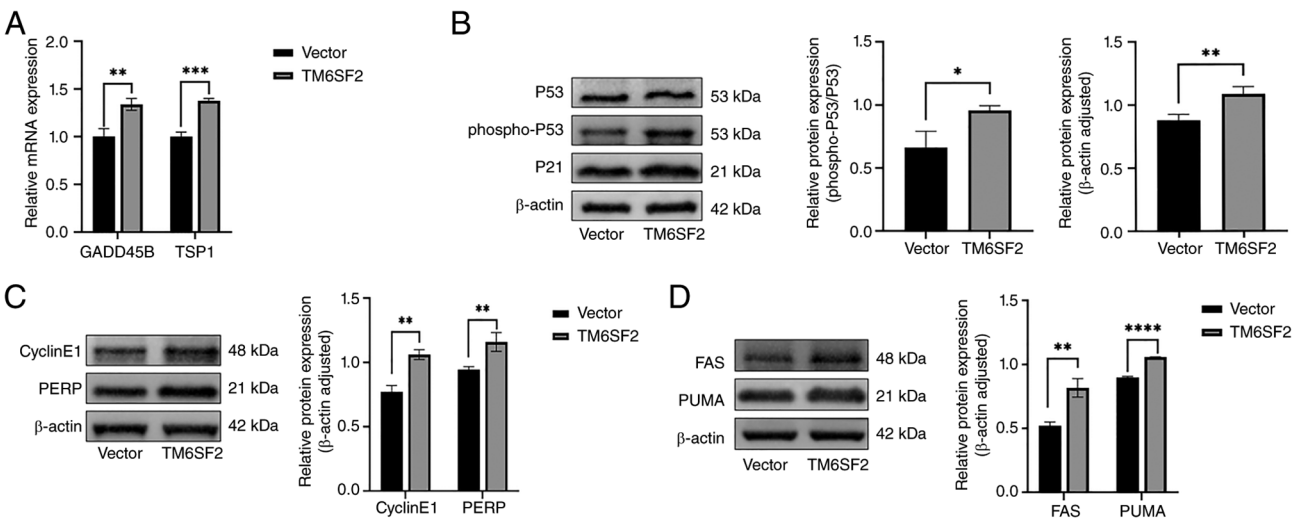

Figure 8. Validation of candidate genes. (A) mRNA expression of genes related to DNA damage-response and angiogenesis-related signaling. (B and C) Protein expression of p53, p21, Cyclin E1 and (PERP). (D) Protein expression of pro-apoptotic proteins (FAS) and (PUMA). Experiments were repeated three times. *P<0.05, **P<0.01, ***P<0.001 and ****P<0.0001 vs. control Vector group. p53, tumor protein p53; p21, cyclin-dependent kinase inhibitor 1A; Cyclin E1, cyclin E1; PERP, p53 apoptosis effector related to PMP22; FAS, Fas cell surface death receptor; PUMA, p53 upregulated modulator of apoptosis.

markedly induced S-phase cell-cycle arrest and apoptosis in HCC cells. These findings are partially consistent with the transcriptome sequencing results showing alterations in genes annotated to the p53 signaling pathway.

Functional enrichment analysis showed that TM6SF2-associated genes were enriched in the p53 signaling pathway, suggesting that p53-related molecular changes may be associated with TM6SF2-induced alterations in cell-cycle distribution and apoptosis (24,25). To further explore this possibility, phosphorylated p53 and selected p53-related downstream molecules were assessed in TM6SF2-overexpressing Huh-7 cells.

p53 is a well-established tumor suppressor that regulates cell-cycle arrest, apoptosis, the DNA damage response, and other tumor-suppressive processes. Under basal conditions, p53 protein levels are tightly controlled. In response to cellular stress, phosphorylation of p53 can reduce its interaction with MDM2/MDMX, increase its stability, and promote the transcriptional activation of downstream target genes (26). In the present study, although RNA-Seq analysis revealed changes in

genes within the p53 pathway, the most functionally relevant finding was the increased level of phosphorylated p53 protein in TM6SF2-overexpressing cells. This result suggested p53-related post-translational molecular changes.

Consistently, the p21 protein levels, a key downstream target of p53, were increased in the TM6SF2 group. p21 is a downstream effector of p53 and is involved in cell-cycle arrest by regulating cyclin-CDK activity. Therefore, increased p21 expression may be associated with TM6SF2-induced S-phase cell-cycle arrest. The apparent discrepancy between changes in TP53 transcript levels and increased phosphorylated p53 protein may be explained by post-translational regulation and feedback control within the p53 signaling pathway. Thus, increased p-p53, rather than TP53 mRNA expression alone, was considered the main evidence of p53-related molecular changes in this study.

In the present study, the expression levels of apoptosis-related proteins, including p53 upregulated modulator of apoptosis (PUMA) and Fas cell surface death receptor (FAS), were increased following TM6SF2 overexpression. p53 apoptosis effector related to PMP22 (PERP), another p53-related apoptotic regulator, was also upregulated in TM6SF2-overexpressing cells. These results suggested that TM6SF2 overexpression may promote apoptosis in Huh-7 cells and that p53-related apoptotic regulators may be associated with this process (27-29).

The cell cycle is a key process that regulates cell fate and its dysregulation is a hallmark of cancer, leading to uncontrolled tumor cell proliferation (30). Cell-cycle regulators are therefore closely associated with cancer development and progression (31). p21, an important cell-cycle regulatory protein, coordinates cell-cycle progression, DNA replication, and DNA repair by inhibiting CDK activity, thereby linking tumor suppression to cell-cycle control (32,33). In the present study, TM6SF2 overexpression significantly increased the proportion of cells in S phase, decreased the proportion of cells in G_1 phase but had no significant effect on the G_2/M phase. These results suggested that TM6SF2 induces S-phase cell-cycle arrest rather than accelerating the G_1/S transition. The decrease in G_1-phase cells may therefore be a consequence of cell accumulation in S phase. Although cyclin E1 is an important regulator of the G_1/S transition (34), the increased S-phase population observed in the present study should be interpreted primarily as S-phase arrest rather than enhanced cell-cycle progression.

At the molecular level, TM6SF2 overexpression was accompanied by increased levels of phosphorylated p53 and p21. p21 is an important cell-cycle regulator and downstream effector of p53 that is involved in cell-cycle arrest by regulating cyclin-CDK activity (32,33). Therefore, increased p21 expression may contribute to TM6SF2-induced S-phase arrest. In addition, the upregulation of GADD45B may indicate activation of DNA damage-response-related processes, which may further contribute to S-phase arrest and apoptosis in Huh-7 cells (35,36). However, further experiments are required to determine whether these molecular changes are required for TM6SF2-induced S-phase arrest and apoptosis.

TM6SF2 overexpression also promoted apoptosis in Huh-7 cells. Consistently, the expression levels of p53-related apoptotic regulators, including PERP, FAS and PUMA, were increased following TM6SF2 overexpression. These findings suggested that p53-related apoptotic regulators may be associated with TM6SF2-mediated inhibition of Huh-7 cell growth.

In addition, the altered expression of TSP-1, an anti-angiogenic factor regulated by p53 (37), suggests that TM6SF2 may also be associated with angiogenesis-related signaling. However, this conclusion is based on changes in gene expression, and further functional experiments are required to confirm whether TM6SF2 directly affects angiogenesis or metastasis.

In summary, the results of the present study suggested that TM6SF2 overexpression affects genes involved in cell-cycle regulation, apoptosis, DNA damage-response-related processes and angiogenesis-related signaling. These changes were accompanied by alterations in p53-related molecular markers. Therefore, TM6SF2 may exert anti-tumor effects in Huh-7 cells, while the involvement of p53-related signaling in this process requires further functional validation.

The present study had several limitations. First, the functional experiments were performed only in Huh-7 cells, which limits the generalizability of the findings to other HCC cell models. Second, Huh-7 cells harbor mutant p53; therefore, the potential involvement of p53-related molecular changes in TM6SF2-mediated effects should be further validated in additional HCC cell lines with different p53 statuses, such as HepG2 and Hep3B. Third, the present study did not include *in vivo* experiments or functional rescue experiments, such as p53 inhibition or knockdown. Therefore, whether p53-related molecular changes are required for TM6SF2-induced S-phase arrest and apoptosis remains to be investigated. Finally, although RNA-Seq and KEGG enrichment analyses provide preliminary mechanistic clues, additional validation is needed to confirm the downstream pathways regulated by TM6SF2. In addition, although additional TCGA-based analyses were performed, TM6SF2 expression was not identified as an independent prognostic factor in the multivariate Cox regression model; therefore, its clinical prognostic value requires further validation in independent cohorts.

In summary, the results of the present study suggested that TM6SF2 overexpression inhibited proliferation, migration, and invasion, while inducing S-phase cell-cycle arrest and apoptosis in Huh-7 cells. RNA-Seq and pathway enrichment analyses indicated that p53-related genes were altered following TM6SF2 overexpression. Increased levels of phosphorylated p53 and p21 proteins further suggest that p53-related molecular changes were associated with TM6SF2 overexpression. These findings provide preliminary evidence that TM6SF2 may function as a tumor suppressor in HCC cells; however, further validation in additional cell models and *in vivo* systems is required.

Acknowledgements

The authors thank Dr Yiqiang Zhao from China Agricultural University, Beijing, China, for helpful suggestions regarding statistical methods.

Funding

The present study was supported by the Excellent Young Teachers Training Program of Higher Education Institutions

of Anhui Province (grant no. YQYB2024039), the Key Project of Natural Science Foundation of Anhui Provincial Department of Education (grant nos. 2025AHGXZK30776, 2025AHGXZK31423 and KJ2020A0591), the Anhui Province Key Laboratory of Immunology in Chronic Diseases (grant no. MBZZ202403), the Open Project of Anhui Province Key Laboratory of Basic and Translational Research of Inflammation-related Diseases (grant no. YZ2024D02), the Innovation and Entrepreneurship Training Program for College Students (grant nos. 12311410002, 202510367023, 202510367024, Byycx25003 and Bydc2025020) and the Open Competition-based Scientific Research Tackling Program of Bengbu Medical University (grant no. 2025byjbgs009).

Availability of data and materials

The RNA-Seq datasets generated and analyzed during the current study are available in the NCBI Sequence Read Archive repository under BioProject accession no. PRJNA858660 (https://www.ncbi.nlm.nih.gov/bioproject/PRJNA858660). The data generated in the present study may be requested from the corresponding author.

Authors' contributions

YW and HH conceived and designed the study. ZH, WX, XJ, SP, WX and SL performed the experiments and analyzed the data. ZH and WX wrote the original manuscript. YW and HH revised the manuscript. ZH and YW confirm the authenticity of all the raw data. All authors read and approved the final manuscript.

Ethics approval and consent to participate

Not applicable.

Patient consent for publication

Not applicable.

Competing interests

The authors declare that they have no competing interests.

References

1. Vogel A, Meyer T, Sapisochin G, Salem R and Saborowski A: Hepatocellular carcinoma. Lancet 400: 1345-1362, 2022.
2. Bray F, Laversanne M, Sung H, Ferlay J, Siegel RL, Soerjomataram I and Jemal A: Global cancer statistics 2022: GLOBOCAN estimates of incidence and mortality worldwide for 36 cancers in 185 countries. CA: Cancer J Clin 74: 229-263, 2024.
3. Llovet JM, Kelley RK, Villanueva A, Singal AG, Pikarsky E, Roayaie S, Lencioni R, Koike K, Zucman-Rossi J and Finn RS: Hepatocellular carcinoma. Nat Rev Dis Primers 7: 6, 2021.
4. Chen Y, Xue W, Zhang Y, Gao Y and Wang Y: A novel disulfidptosis-related immune checkpoint genes signature: Forecasting the prognosis of hepatocellular carcinoma. J Cancer Res Clini Oncol 149: 12843-1254, 2023.
5. Carim-Todd L, Escarceller M, Estivill X and Sumoy L: Cloning of the novel gene TM6SF1 reveals conservation of clusters of paralogous genes between human chromosomes 15q24-->q26 and 19p13.3-->p12. Cytogenet Cell Genet 90: 255-260, 2000.
6. Choudhary NS and Duseja A: Genetic and epigenetic disease modifiers: Non-alcoholic fatty liver disease (NAFLD) and alcoholic liver disease (ALD). Transl Gastroenterol Hepatol 6: 2, 2021.
7. Kozlitina J, Smagris E, Stender S, Nordestgaard BG, Zhou HH, Tybjærg-Hansen A, Vogt TF, Hobbs HH and Cohen JC: Exome-wide association study identifies a TM6SF2 variant that confers susceptibility to nonalcoholic fatty liver disease. Nat Genet 46: 352-356, 2014.
8. Smagris E, Gilyard S, BasuRay S, Cohen JC and Hobbs HH: Inactivation of Tm6sf2, a gene defective in fatty liver disease, impairs lipidation but not secretion of very low density lipoproteins. J Biol Chem 291: 10659-10676, 2016.
9. Luo F, Smagris E, Martin SA, Vale G, McDonald JG, Fletcher JA, Burgess SC, Hobbs HH and Cohen JC: Hepatic TM6SF2 is required for lipidation of VLDL in a pre-golgi compartment in mice and rats. Cell Mol Gastroenterol Hepatol 13: 879-899, 2022.
10. Holmen OL, Zhang H, Fan Y, Hovelson DH, Schmidt EM, Zhou W, Guo Y, Zhang J, Langhammer A, Løchen ML, *et al*: Systematic evaluation of coding variation identifies a candidate causal variant in TM6SF2 influencing total cholesterol and myocardial infarction risk. Nat Genet 46: 345-551, 2014.
11. Jiang X, Qian H and Ding WX: New glance at the role of TM6SF2 in lipid metabolism and liver cancer. Hepatology 74: 1141-1144, 2021.
12. Anstee QM, Reeves HL, Kotsiliti E, Govaere O and Heikenwalder M: From NASH to HCC: Current concepts and future challenges. Nat Rev Gastroenterol Hepatol 16: 411-428, 2019.
13. Li XY, Liu Z, Li L, Wang HJ and Wang H: TM6SF2 rs58542926 is related to hepatic steatosis, fibrosis and serum lipids both in adults and children: A meta-analysis. Front Endocrinol (Lausanne) 13: 1026901, 2022.
14. Yicun W, Dong X and Huanhua L: Differential expression of TM6SF2 in hepatocellular carcinoma and its effect on the biological behavior of hepatocellular carcinoma cells. Acta Universitatis Medicinalis Anhui. (Chinese) 56: 180-185, 2021.
15. Livak KJ and Schmittgen TD: Analysis of relative gene expression data using real-time quantitative PCR and the 2-ΔΔCT method. Methods 25: 402-408, 2001.
16. Kim D, Paggi JM, Park C, Bennett C and Salzberg SL: Graph-based genome alignment and genotyping with HISAT2 and HISAT-genotype. Nat Biotechnol 37: 907-915, 2019.
17. Pertea M, Pertea GM, Antonescu CM, Chang TC, Mendell JT and Salzberg SL: StringTie enables improved reconstruction of a transcriptome from RNA-seq reads. Nat Biotechnol 33: 290-295, 2015.
18. Love MI, Huber W and Anders S: Moderated estimation of fold change and dispersion for RNA-seq data with DESeq2. Genome Biol 15: 550, 2014.
19. Dikic I and Elazar Z: Mechanism and medical implications of mammalian autophagy. Nat Rev Mol Cell Biol 19: 349-364, 2018.
20. Wang Y, Sheng Z, Wang Y, Li Q, Gao Y, Wang Y, Dai Y, Liu G, Zhao Y and Li N: Transgenic mouse milk expressing human bile salt-stimulated lipase improves the survival and growth status of premature mice. Mol Biotechnol 57: 287-297, 2015.
21. Daly AK, Day CP, Liu YL and Anstee QM: TM6SF2 as a genetic risk factor for fibrosis. Hepatology 62: 1321, 2015.
22. Li TT, Li TH, Peng J, He B, Liu LS, Wei DH, Jiang ZS, Zheng XL and Tang ZH: TM6SF2: A novel target for plasma lipid regulation. Atherosclerosis 268: 170-176, 2018.
23. Xue WY, Zhang L, Liu CM, Gao Y, Li SJ, Huai ZY, Dai J and Wang YY: Research progress on the relationship between TM6SF2 rs58542926 polymorphism and non-alcoholic fatty liver disease. Expert Rev Gastroenterol Hepatol 16: 97-107, 2022.
24. Levine AJ: p53: 800 million years of evolution and 40 years of discovery. Nat Rev Cancer 20: 471-480, 2020.
25. Liu Y, Su Z, Tavana O and Gu W: Understanding the complexity of p53 in a new era of tumor suppression. Cancer Cell 42: 946-967, 2024.
26. Kruse JP and Gu W: Modes of p53 regulation. Cell 137: 609-622, 2009.
27. Wang MJ, Huang HY, Chiu TL, Chang HF and Wu HR: Peroxiredoxin 5 silencing sensitizes dopaminergic neuronal cells to rotenone via DNA damage-triggered ATM/p53/PUMA signaling-mediated apoptosis. Cells 9: 22, 2019.
28. Attardi LD, Reczek EE, Cosmas C, Demicco EG, McCurrach ME, Lowe SW and Jacks T: PERP, an apoptosis-associated target of p53, is a novel member of the PMP-22/gas3 family. Genes Dev 14: 704-718, 2000.

29. Chao C, Saito S, Kang J, Anderson CW, Appella E and Xu Y: p53 transcriptional activity is essential for p53-dependent apoptosis following DNA damage. EMBO J 19: 4967-4975, 2000.
30. Vijayaraghavan S, Moulder S, Keyomarsi K and Layman RM: Inhibiting CDK in cancer therapy: current evidence and future directions. Target Oncol 13: 21-38, 2018.
31. Matsuda Y, Wakai T, Kubota M, Osawa M, Takamura M, Yamagiwa S, Aoyagi Y, Sanpei A and Fujimaki S: DNA damage sensor γ -H2AX is increased in preneoplastic lesions of hepatocellular carcinoma. ScientificWorldJournal 2013: 597095, 2013.
32. Engeland K: Cell cycle regulation: p53-p21-RB signaling. Cell Death Differ 29: 946-960, 2022.
33. Ticli G, Cazzalini O, Stivala LA and Prosperi E: Revisiting the function of $p21^{CDKN1A}$ in DNA repair: The influence of protein interactions and stability. Int J Mol Sci 23: 7058, 2022.
34. Fagundes R and Teixeira LK: Cyclin E/CDK2: DNA replication, replication stress and genomic instability. Front Cell Dev Biol 9: 774845, 2021.
35. Yoo J, Ghiassi M, Jirmanova L, Balliet AG, Hoffman B, Fornace AJ Jr, Liebermann DA, Bottinger EP and Roberts AB: Transforming growth factor-beta-induced apoptosis is mediated by Smad-dependent expression of GADD45b through p38 activation. J Biol Chem 278: 43001-43007, 2003.
36. Prabhu KS, Therachiyil L, Masoodi T, Bhat AA and Uddin S: GADD45: A crucial component of the DNA damage response and a potential cancer therapeutic target. Expert Opin Ther Targets 29: 743-756, 2025.
37. Ren B, Yee KO, Lawler J and Khosravi-Far R: Regulation of tumor angiogenesis by thrombospondin-1. Biochim Biophys Acta 1765: 178-188, 2006.